International Journal of Mining Science and Technology 32 (2022) 1021–1029

Contents lists available at ScienceDirect

International Journal of Mining Science and Technology

journal homepage: www.elsevier.com/locate/ijmst

An investigation of machine learning techniques to estimate minimum horizontal stress magnitude from borehole breakout

Huasheng Lin [a], Sarvesh Kumar Singh [b], Zizhuo Xiang [b], Won Hee Kang [c], Simit Raval [b], Joung Oh [b,*], Ismet Canbulat [b]

[a] Glencore Coal Assets Australia, Mount Thorley 2330, Australia
[b] School of Minerals and Energy Resources Engineering, University of New South Wales, Sydney 2052, Australia
[c] Centre for Infrastructure Engineering, School of Engineering, Western Sydney University, Penrith 2751, Australia

ARTICLE INFO

Article history:
Received 16 August 2021
Received in revised form 21 December 2021
Accepted 15 June 2022
Available online 25 June 2022

Keywords:
Borehole breakout
In-situ stress estimation
Comparative analysis
Machine learning

ABSTRACT

Borehole breakout is a widely utilised phenomenon in horizontal stress orientation determination, and breakout geometrical parameters, such as width and depth, have been used to estimate both horizontal stress magnitudes. However, the accuracy of minimum horizontal stress estimation from borehole breakout remains relatively low in comparison to maximum horizontal stress estimation. This paper aims to compare and improve the minimum horizontal stress estimation via a number of machine learning (ML) regression techniques, including parametric and non-parametric models, which have rarely been explored. ML models were trained based on 79 laboratory data from published literature and validated against 23 field data. A systematic bias was observed in the prediction for the validation dataset whenever the horizontal stress value exceeded the maximum value in the training data. Nevertheless, the pattern was captured, and the removal of systematic bias showed that the artificial neural network is capable of predicting the minimum horizontal stress with an average error rate of 10.16% and a root mean square error of 3.87 MPa when compared to actual values obtained through conventional in-situ measurement techniques. This is a meaningful improvement considering the importance of in-situ stress knowledge for underground operations and the availability of borehole breakout data.

1. Introduction

The increased national and global demand for mineral resources has caused underground explorations to go deeper, which has raised serious health and safety concerns [1]. As a result, the knowledge of in-situ stress is becoming increasingly critical for the design and safety of underground operations. At present, the most frequently used stress measurement techniques are overcoring and hydraulic fracturing [2]. However, these techniques are only applicable to intact borehole walls where surrounding rock in the tested borehole sections needs to be elastic [2,3]. This is difficult to be achieved in weak strata. Borehole breakout is a drilling-induced phenomenon that has been utilised as an indication tool for horizontal stress magnitudes and orientation [4-6]. A schematic figure of borehole breakout can be seen in Fig. 1. L represents the maximum breakout depth and R represents the borehole radius. Breakout depth is usually expressed as a ratio due to various borehole sizes. Its geometries, breakout depth (L/R) and width (θ_b), are argued to be dependent on in-situ stress environment [7-9]. In the past decades, a series of studies attempted to derive horizontal stress magnitudes from breakout geometries with analytical approaches [4,5,10-12], experimental investigations [13] and numerical modelling [6,14-18]. Field experiments were also conducted to study the breakout development, its relationship with in-situ stress magnitudes, and spalling phenomenon [19-23]. However, there has not been a universally accepted method developed to date. Knowing a determined minimum horizontal stress value is pivotal to underground excavation design, as it governs the potential rock failure state. Conventional methods such as stress polygon [5,10] provide a broad range of horizontal stress magnitudes, which is not sufficient for design purposes. Therefore, this study aims to investigate machine learning (ML) models to provide a reliable single value output.

The recent advancements in sensing, consistent data collection, and reliable data processing have assisted modern-day civil and mining operations in combining industrial, laboratory, and numerical research through computer-aided programs. Particularly, ML

* Corresponding author.
E-mail address: joung.oh@unsw.edu.au (J. Oh).

https://doi.org/10.1016/j.ijmst.2022.06.005
2095-2686/

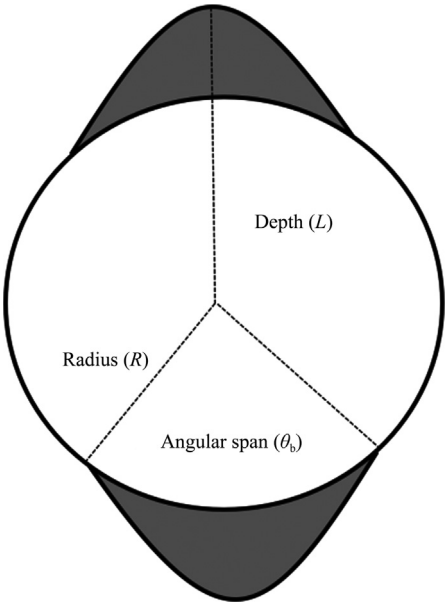

Fig. 1. Illustration of borehole breakout (after [24]).

has seen a greater influence on prediction and regression tasks due to its ability in capturing linear and complex non-linear relationships between independent variables and the dependent target. ML models such as an artificial neural network (ANN) have already been demonstrated in predicting parameters such as surface roughness, using limited training data (less than100 data points), which provided critical information for improving the quality of support structures [25,26]. Similarly, a combination of fuzzy logic and neural network was shown to predict the penetration rate of tunnel boring machines using a limited dataset of rock properties and machine design parameters [27-29]. The comparison of results exhibited substantial improvement over other statistical and empirical approaches. Elmo and Stead [30] provided a critical discussion on the importance of ML in rock mechanics and concluded that it can be an effective tool in studying rock engineering design problems. Lin et al. [31] investigated ANN along with rock failure criterion for estimating horizontal stress magnitudes. The proposed ANN-Mogi-Coulomb technique was able to improve the accuracy of maximum horizontal principal stress (σ_h) estimation while providing reasonable estimation on minimum horizontal stress principal (σ_h) at 15.88% average error rate.

ML models can be divided into parametric learning models and non-parametric learning models [32]. A parametric learning model summarises data with a defined set of parameters that are independent of the number of training samples [33]. A function form is initially decided, the coefficient of which are computed from the training samples. Due to the constrained function form, the parametric models are more suited to solve simpler problems. Benefits of parametric models include low training data requirement, easier result interpretability, and simpler parameter sensitivity analysis. Moreover, it is easier to improve results accuracy to some extent through minor tweaking in the defined function form. Examples of parametric models include linear regression [34], lasso regression [35], ridge regression [36], logistic regression [37], and Naive Bayes classifier [38]. In contrast, the non-parametric models seek to best fit the training samples to construct the mapping function whilst maintaining the ability to generalize the previously unseen data. The models can incorporate many functional forms and can produce high performance; however, a large amount of training samples is required for learning, and there are instances of overfitting. Prominent non-parametric models include k-nearest neighbours [39], decision trees [40], random forest [41], support vector machines [42], Gaussian process regression [43] and artificial neural network [44]. This study investigates both parametric and non-parametric ML models to evaluate performance in predicting minimum horizontal stress under limited training data.

Reliable estimation of σ_h magnitude based on borehole breakout data has been a challenging topic in the past 40 years using the conventional rock mechanics approach. However, the problem itself is a classical prediction and regression which can be solved effectively using ML techniques. Although the method proposed by Lin et al. [31] provides reasonable estimation results, it does not compare available machine learning algorithms to assess accuracy on σ_h prediction. Since there are numerous ML models with their own merits and demerits, they need to be tested on available borehole breakout data for suitability in predicting minimum horizontal stress based on selected borehole parameters. In this study, a comparative analysis of some widely adopted ML techniques on the estimation of minimum horizontal stress from borehole breakout data was carried out. The evaluated ML algorithms, both parametric and non-parametric, include linear regression, lasso regression, ridge regression, classification and regression tree (CART), random forest, support vector machine (SVM), Gaussian process regression (GPR) and artificial neural network (ANN). The comparison result will help determine the most reliable ML technique that can be adopted for future assessments.

2. Methodology

2.1. Breakout data collection

Lin et al. [31] tested the ML model (ANN) based on 79 laboratory training data and validated it against 23 field test data. The training data were collected from experiments conducted by Herrick and Haimson [7], Haimson and Lee [8], Lee et al. [9] and Lin et al. [24,31], and the validation data are from Zoback et al. [4], Walton et al. [45], Shen [46], Klee et al. [47], Shen and Rinne [48], LeRiche [49], and Lin et al. [15]. The parameters used for prediction were: breakout width (θ_b), vertical stress (σ_v) and borehole wall strength (*BWS*). *BWS* was defined by Walton et al. [45] and LeRiche [50] to represent breakout initiation stress at various borehole sizes, which in turn governs the size of breakout geometries. As observed in numerous laboratory studies [24,50,51], breakout geometries were not only influenced by stress conditions and mechanical properties of rock, but also the size of borehole. Therefore, the term *BWS* was introduced to address such stress elevation required for breakout initiation. *BWS* was obtained from source data using conversion relationship given in [15,51]. In both training and validation datasets, borehole breakout geometries were measured by averaging the breakout geometrical profiles along the borehole axis and therefore are assumed to be unbiased and accurate.

2.2. Regression analysis using parametric and non-parametric machine learning models

The parametric ML models utilised in this study include linear regression, lasso regression, and ridge regression. Before training the models, the σ_h was plotted against the 3 variables to observe the distribution and determine Pearson's correlation coefficients between the target and predictors as shown in Fig. 2. The red lines in the figure indicate the best linear fit. A linear fit is shown in red to provide insights on data distribution for better visualisation. The correlation coefficients observed in the training dataset between

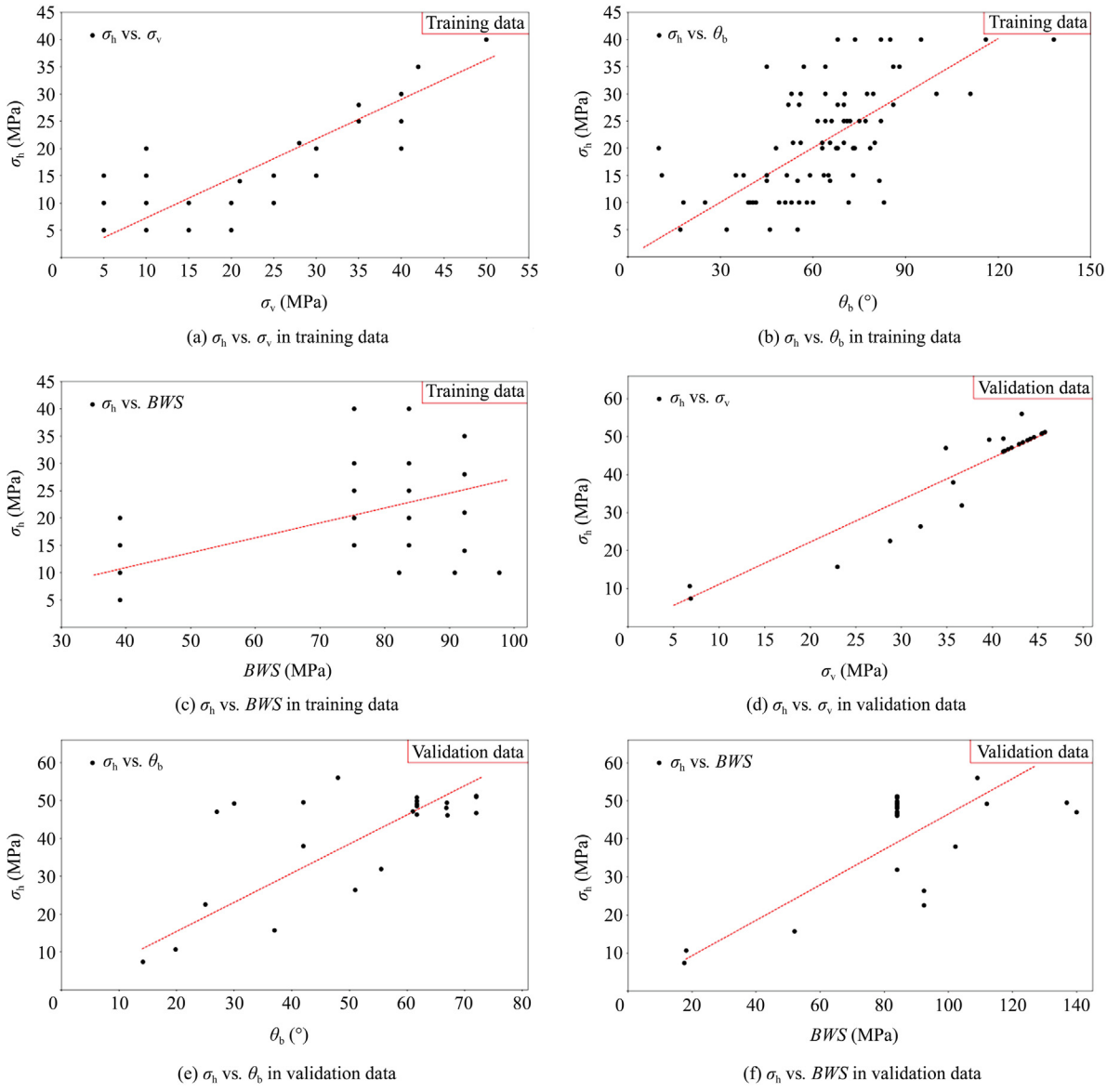

Fig. 2. Visualisation of target vs. predictor data.

σ_h and the 3 variables σ_v, θ_b and *BWS* were 0.89, 0.61 and 0.38, respectively. Correspondingly, in the validation dataset, the observed correlation coefficients were 0.94, 0.69 and 0.69, which was comparatively higher than the training data. Since a low correlation was observed between σ_h and the 2 variables θ_b and *BWS* in the training dataset, additional interaction terms were introduced in the parametric models by multiplying the variables amongst themselves to improve the performance. The interaction terms were first statistically tested for significance in linear regression using *t* statistics and *p* values, then the more significant interaction terms were used in the parametric modelling. The null hypothesis assumed that the coefficient corresponding to a predictor is zero. Table 1 provides the predictor coefficients for linear regression and corresponding *t*-stat and *p* values. For 95% confidence ($t_{1,99}$), the interaction term $\theta_b \times BWS$ seemed insignificant due to its low *t* value. The results were also verified using *p* values, where for 5% significance (p=0.05), and $\theta_b \times BWS$ was substantially high. Hence, the null hypothesis was accepted showing $\theta_b \times BWS$ is insignificant for the model. Therefore, during the training of parametric models, apart from 3 main predictors, two other statistically significant interaction terms $\sigma_v \times \theta_b$ and $\sigma_v \times BWS$ were used. The parametric models such as linear regression, lasso regression (also known as elastic net), and ridge regression were trained and tested with and without the use of the interaction terms. To better regularize and generalize the model, 30% of input samples were used for cross-validation in lasso and ridge regression.

For non-parametric methods, prominent models such as CART, random forest, SVM, GPR, and ANN were examined. In contrast to the parametric models, the non-parametric models were trained without the use of interaction terms as they implicitly account for interactions due to the universal form function. However, modelling in such a case requires the definition of several hyperparameters which were determined from experience and trial and error by keeping consistency over all the methods used in this study, instead of fine-tuning the parameters that just focus on one specific method for a comparison purpose. In this study, hyperparameters defined for CART were minimum number of parent nodes (10), minimum leaf size (4), and maximum splits (78); for random forest were leaf size (8) and number of trees (100); for SVM was kernel type (linear and Gaussian) and epsilon value (1.15); for GPR was

Table 1
Statistical analysis of interaction terms through a linear fit model.

Parameter	Coefficient	Standard error (SE)	*t*-stat	*p* value
Intercept	12.030	5.260	2.290	0.025
$\boldsymbol{\sigma_v}$	−0.320	0.250	−1.290	0.202
$\boldsymbol{\theta_b}$	−0.090	0.120	−0.760	0.450
BWS	0.024	0.080	0.310	0.760
$\sigma_v \times \theta_b$	0.006	0.002	3.950	≈0.000
$\sigma_v \times BWS$	0.006	0.003	2.330	0.023
$\theta_b \times BWS$	−0.001	0.002	−0.660	0.510

kernel type (exponential) and optimizer type (Quasi-Newton), and for ANN was number of hidden layers (1), number of hidden neuron (26) and backpropagation algorithm (Bayesian regularisation). For ANN, the training data was split into training (70%), validation (15%), and test dataset (15%), and the network which resulted in the minimum error in the 3 datasets were selected as the final test model. It is important to note that the mentioned models were implemented with a range of hyperparameters and they exhibit similar behaviour over a particular range. The values listed in the brackets are corresponding to the results shown in this study. The accuracy of the models was evaluated in terms of standard parameters root mean square error (RMSE), maximum absolute error (MAE), and mean percentage error computed by comparing the actual and predicted value on both training and validation datasets. MAE represents the maximum of absolute errors observed in each prediction. The mean percentage error was calculated by taking the average of percentage errors observed in individual observations.

3. Results

3.1. Performance on training data

Post-training, the accuracy was evaluated on both training and test datasets by comparing the predicted and actual values. Table 2 denotes the accuracy of the models achieved on the training and the validation dataset calculated in terms of RMSE, MAE, and mean percentage error. The parametric models such as linear, lasso, and ridge have a relatively higher RMSE than non-parametric models on the training dataset as the predictors were not necessarily independent. Hence, it was essential to incorporate the interaction terms in the parametric model to reduce RMSE. For the training dataset, the least RMSE (1.17 MPa) was observed in GPR with MAE in observations not exceeding 4.49 MPa. However, the GPR resulted in a relatively higher error in the validation dataset due to overfitting. In the validation dataset, CART displayed minimum RMSE (10.47 MPa), although the MAE was least in the case of ANN. For any prediction application, it is necessary to have the least RMSE as well as low MAE in individual observation. For instance, a model may have low RMSE but some of the observations may exhibit high absolute error. Selecting such a model may not always provide a reliable estimate. The top 6 models in terms of performance on the training dataset are shown in Fig. 3. The GPR, CART, and SVM with Gaussian kernel fitted well on training data and exhibited RMSE less than 3 and MAE less than 10, indicating that the error in prediction on the training dataset never exceeds 10 MPa.

3.2. Model fitting on validation data

Fig. 4 shows the actual vs. predicted value for the best 6 models based on the RMSE in the independent validation dataset. The models exhibit relatively accurate fitting when the stress is below 30 MPa, and a systematic bias was seen between the predicted and actual values of σ_h whenever the actual σ_h value exceeded 40 MPa. It is important to note that the maximum σ_h value in the training dataset was 40 MPa. The maximum and minimum value of the target and the predictors in the training and validation dataset is shown in Table 3. The predictor values in the validation dataset, except *BWS*, are always within the range of training data and never exceed it. Also, σ_v and θ_b show a comparatively higher correlation (0.89 and 0.61, respectively) with σ_h than *BWS* (0.38) in training data. As such the weight assigned by ML models are higher for σ_v and θ_b due to better correlation when compared to *BWS*. Therefore, it is difficult for ML models to predict something which goes substantially beyond the range of σ_h values present in the training data due to the lower weight coefficient of *BWS*. The prediction values are always less than the actual values whenever actual σ_h>40-MPa. Nevertheless, the pattern in the data is captured by the majority of models except for CART (Fig. 4), and there is always a bias in the prediction for actual σ_h>40 MPa which corresponds to predicted σ_h>23 MPa. Most of the models have different fits on

Table 2
Error evaluation of ML models in predicting minimum horizontal stress (σ_h).

Machine learning model	Training			Validation			Validation after removing bias		
	RMSE (MPa)	MAE (MPa)	Mean error (%)	RMSE (MPa)	MAE (MPa)	Mean error (%)	RMSE (MPa)	MAE (MPa)	Mean error (%)
Linear regression	4.50	7.75	22.57	16.50	25.73	34.51	5.14	11.52	13.41
Linear regression (with interaction)	3.82	8.55	19.95	15.31	20.24	34.71	4.95	7.11	15.75
Lasso regression	5.02	11.99	25.11	17.94	27.26	35.08	8.17	22.64	17.00
Lasso regression (with interaction)	4.10	11.13	20.14	16.55	24.56	32.45	5.08	10.54	11.34
Ridge regression	4.40	12.95	21.94	16.98	26.40	35.13	6.22	12.99	15.51
Ridge regression (with interaction)	3.97	10.32	20.58	16.11	24.28	31.57	4.77	10.33	10.76
CART	2.29	7.50	11.55	10.47	21.00	23.01	5.20	12.76	12.02
Random forest	3.49	9.19	18.94	17.86	28.11	33.50	10.54	25.92	21.97
SVM linear kernel	4.54	16.00	20.71	15.87	24.21	37.34	5.31	10.66	17.29
SVM linear kernel (with interaction)	3.88	9.00	20.51	14.74	20.31	28.87	4.60	8.62	10.55
SVM Gaussian kernel	2.90	9.89	12.66	14.79	23.94	36.64	7.44	23.21	20.84
GPR	1.17	4.49	4.81	15.97	21.14	26.21	4.97	7.39	15.40
ANN	3.29	9.77	15.73	12.20	17.17	25.33	3.87	6.68	10.16

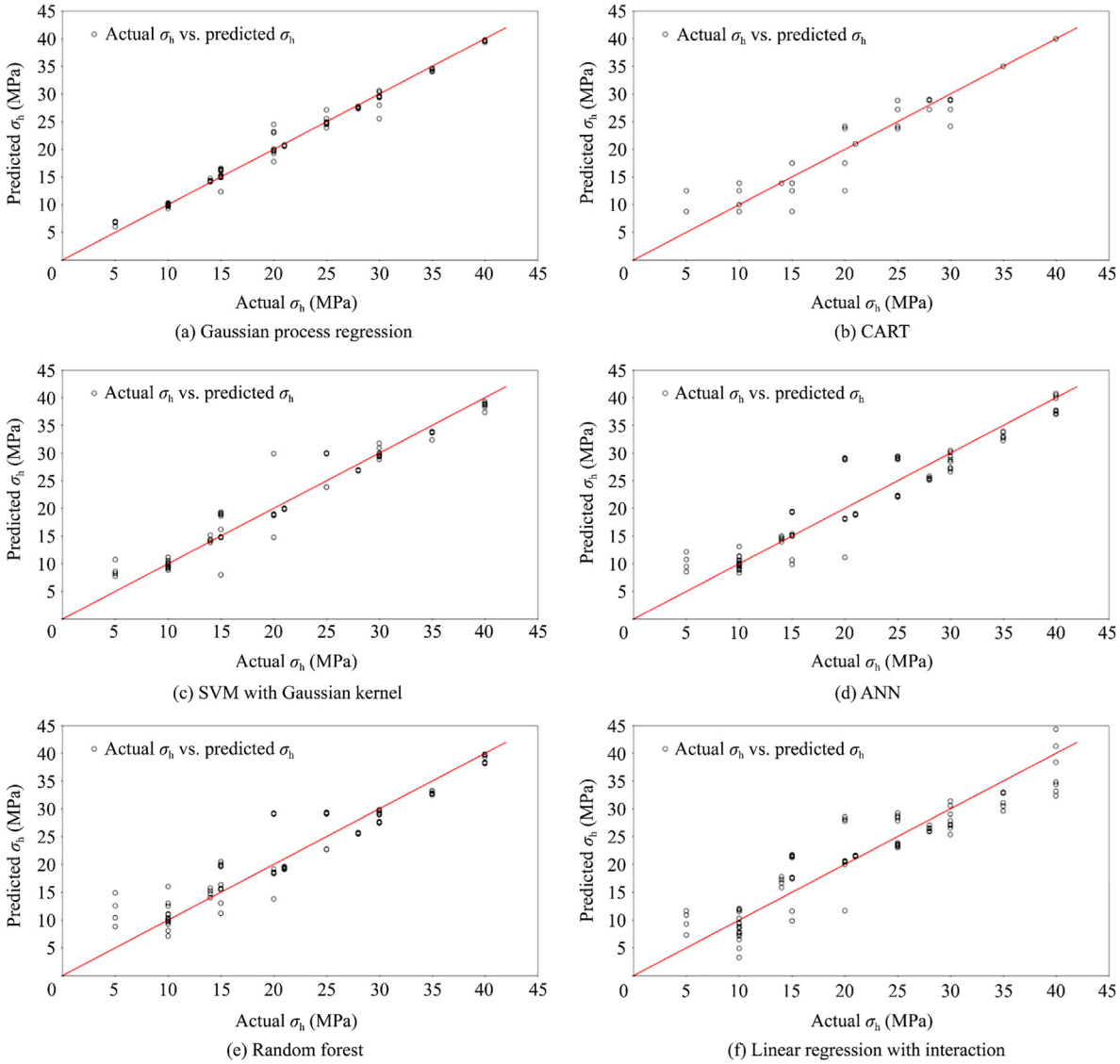

Fig. 3. Prediction vs. actual value comparison resulting from various ML algorithms for training data.

the data and hence the pattern varies. Some of the models captured the pattern better than the others which can be visually observed in the actual and predicted values (Fig. 4). In some ML models such as ANN, GPR, and linear SVM, the bias in predicted value is systematic, while in the other models, there is a slight variation in observed bias based on the defined model. It is possible to account for the systematic bias by taking the mean of the difference between the actual and predicted values for actual σ_h>40 MPa and adding it to the predicted value whenever predicted σ_h>23-MPa. A systematic bias term is introduced to re-adjust the output of the training to obtain a more accurate model.

Fig. 5 shows the result of the best 6 models after the removal of systematic bias. The accuracy of the models after removing bias is presented in Table 2 in the last 3 columns. Parametric models such as linear, lasso, and ridge regression did not achieve optimal performance due to fixed form function, however, the introduction of interaction terms increased the accuracy though the MAE was still high. Some non-parametric models such as regression tree, random forest, and SVM with Gaussian kernel had a problem of overfitting, and there was a large difference between training accuracy and validation accuracy. SVM with linear kernel function had a better data generalisation than the SVM with Gaussian kernel and led to low validation error while sufficiently capturing the pattern. In general, the selection of kernel for SVM is more based on prior data information. GPR had a similar performance as SVM with a linear function, although the observed MAE was less than that of SVM. ANN provided the best results with an RMSE of 3.87 and an MAE of 6.68 in the prediction. The training of ANN requires a trial-and-error process with a variable number of neurons and different backpropagation training algorithms such as scaled conjugate gradient, Bayesian regularization, etc. In this study, the best performance was obtained for 26 neurons and Bayesian regularization backpropagation. Higher prediction accuracy is obtained for ANN, as during training, a better generalisation is achieved by subsequently dividing the training data into training, test and validation sets, and minimising the error in all 3 of them. Hence, whenever new data is encountered, the model tends to perform better.

4. Discussion

In parametric models, ridge regression has slightly better performance than linear and lasso regression due to regularisation of parameters, i.e., the coefficient of the independent variable, is

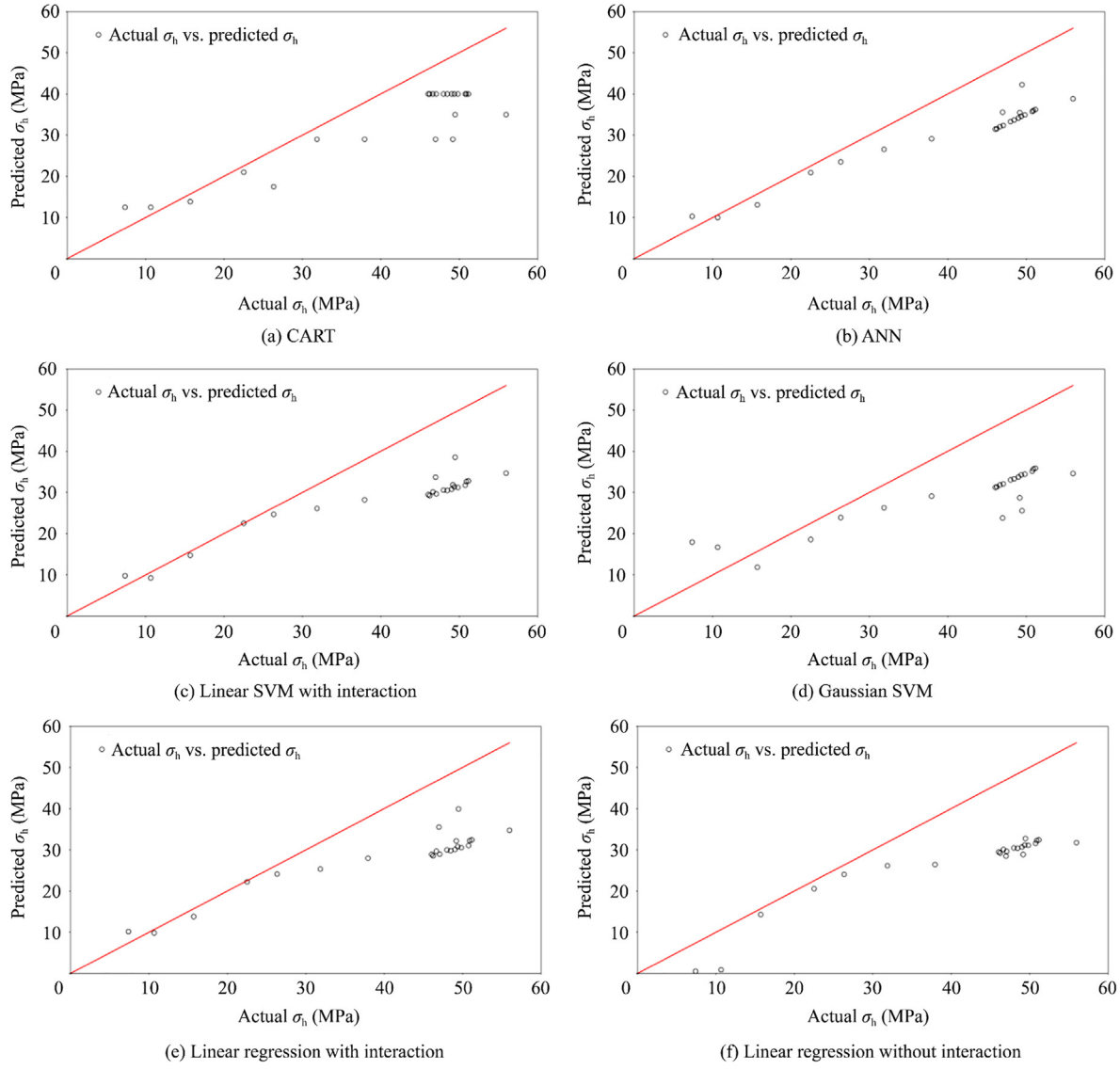

Fig. 4. Predicted vs. actual value comparison resulting from various ML algorithms for validation data.

Table 3
Maximum and minimum values of variables in training and validation datasets.

Variable	Training data		Validation data	
	Max	Min	Max	Min
σ_h (MPa)	40.00	5.00	56.00	7.39
σ_v (MPa)	50.00	5.00	45.78	6.78
θ_b (°)	138.00	10.00	72.00	14.17
BWS (MPa)	97.72	39.08	140.00	17.61

done such that any particular variable does not influence the output considerably. Among non-parametric models, CART had the best performance quantitatively when the systematic bias was not considered. CART algorithm uses least error. However, upon visual interpretation (Fig. 4), it was found that CART does not recognise any pattern for predicted σ_h>23 MPa when compared to other models. The output of regression trees is sensitive to the hyperparameters such as maximum depth of the tree, number of nodes, splits, etc., and the model often suffers from overfitting leading to inaccurate predictions and patterns [40]. A systematic bias was observed for a few validation data points where the actual values of minimum horizontal stress were comparatively higher than what was given in the training data. The prediction curve in Fig. 4 shows that there is a somewhat constant bias between the estimated and actual values. While it is possible to model it, a constant value was used to reduce the error between actual and estimated values, and to avoid overfitting, which may lead to unreliable results for new field data. After removing systematic bias, the predicted error reduced considerably, and the best results were achieved for non-parametric models SVM (with linear kernel), GPR, and ANN. SVM with Gaussian kernel had overfitted on training data which affected its performance on the validation dataset, whereas the use of linear kernel had a better data fitting, exhibiting a somewhat linear trend in the data. Most of the super-

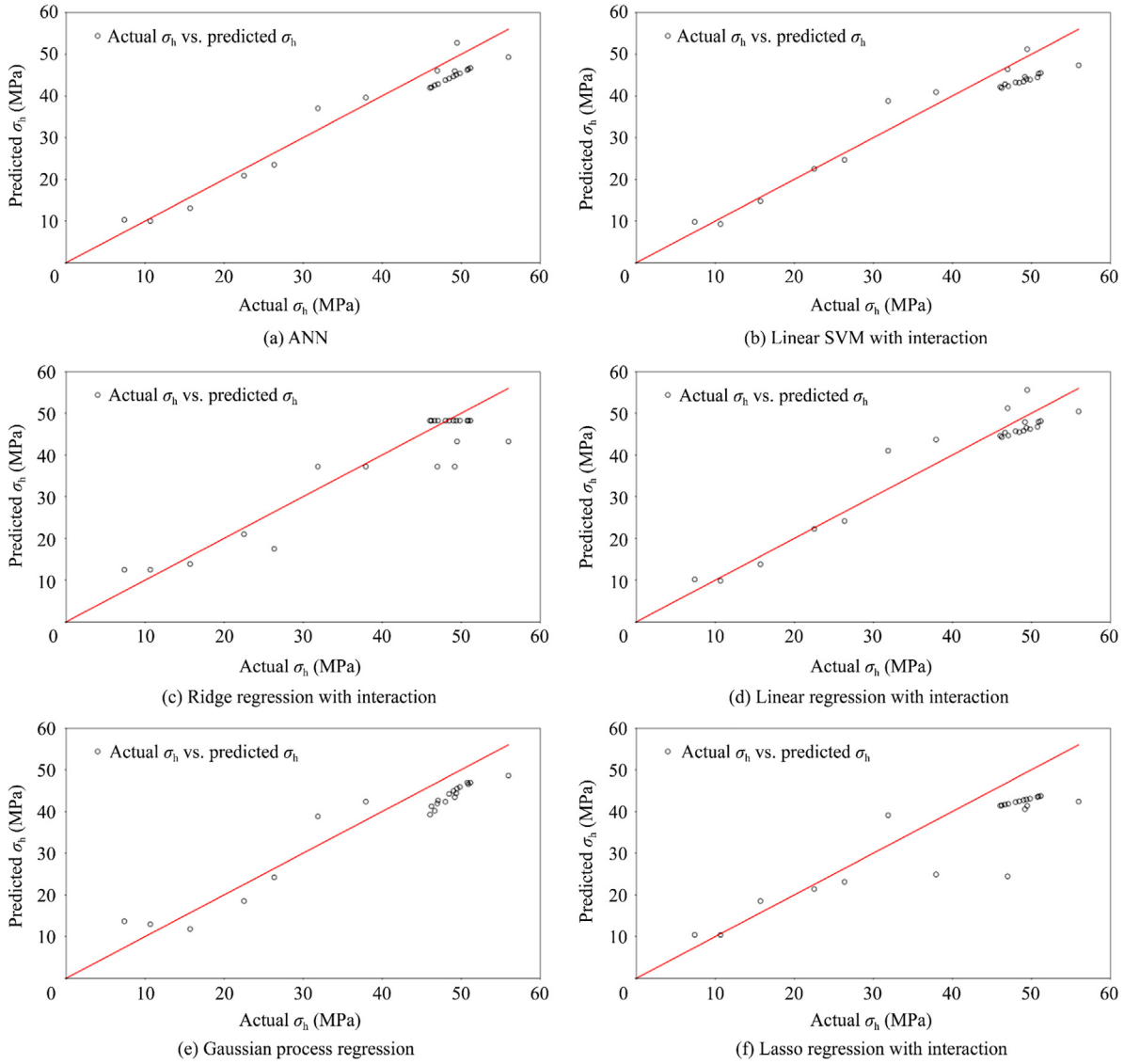

Fig. 5. Comparison of predicted and actual σ_h values for various ML models after removing systematic bias.

vised ML models mentioned above learn exact values of parameter coefficients in a function for prediction, and the choice of wrong coefficients often lead to misleading prediction. A Gaussian process regression (GPR) avoids such issues by using a Bayesian approach that infers a probability distribution over all possible coefficients and relocates the probabilities based on evidence. Therefore, GPR resulted in the second-best performance when both RMSE and MAE were analysed. Moreover, GPR is known to work well on small datasets and can provide uncertainty measurements on the predictions [43]. Among all analysed models, ANN resulted in the least error. The ability of ANN to use a network of interconnected neurons lets it learn from the data while subsequently checking for generalisation through random data partition for the best possible result. Therefore, the ANN model performs better than the rest on previously unseen data.

The parametric models used in the study exhibited higher RMSE error in the absence of interaction terms. Since the parametric model has a fixed form function, the interaction terms are automatically ignored. Therefore, these terms must be tested statistically for their significance while training the model for improving performance. The non-parametric models such as ANN and decision tree have a universal function form, and they implicitly take into account the interaction term while modelling. However, the non-parametric model often overfits the training data, resulting in low prediction accuracy in the validation dataset. Moreover, the selection of hyperparameters plays a critical role and a small change may severely affect model performance. For instance, a large difference in RMSE can be seen for SVM when a kernel function is changed from linear to Gaussian although the Gaussian function has a better fit on training data. Nevertheless, machine algorithms can identify the patterns in the data to provide a more reliable estimate.

It is important to note that more parameters, incorporating surrounding rock properties, may improve prediction results. However, it is difficult to obtain such parameters in the field and analysis mostly ends up making assumptions. Nevertheless, variable rock properties across 79 training and 23 validation data, resulting from different experimental scenarios and field conditions, were captured in terms of the *BWS* parameter which incorporates UCS and borehole size effect. This study chose the 3 parameters based on their relevance and simplicity in obtaining from borehole breakout. The influence of the unknown parameters that may be relevant in predicting σ_h is included in the prediction error. The small error in the ML outputs indicates that the use of the 3 practically available input parameters effectively contributes to the prediction.

The output of ML models depends on the quality and number of training data, and the dataset must capture the existing pattern to provide the optimal output. Conducting a borehole breakout experiment is a timely process with constraints on laboratory equipment. A true tri-axial machine is required for such experiments which should be capable of applying high stress magnitudes from all directions. Drilling a borehole under such a high-stress environment is even more challenging. Due to these difficulties, there have been only limited borehole breakout experiments carried out in the world. The accuracy of the ML models could be enhanced by removing outliers or increasing the number of training samples. However, any potential errors in the training and validation datasets used in this study are hard to detect and remove since experimental biases are inconceivable from published literature. Therefore, the authors are trying to enrich the database by conducting more experiments for highly reliable outputs.

5. Conclusions

This paper presented a comparative analysis of popular ML techniques on the estimation of σ_h using borehole breakout. The findings and conclusions are summarised below point-by-point:

(1) *BWS* parameter has a comparatively lower correlation (0.38) to σ_h than σ_v (0.89) and θ_b (0.61) for training data. Whereas all the parameters show relatively higher correlation on the validation data (*BWS*: 0.69, σ_v: 0.94 and θ_b: 0.69).
(2) In total, 13 different models were developed and validated using 79 experimental and 23 field data. Among all ML techniques, the ANN model yielded the most accurate estimation results on field data, with a mean error rate of 10.16% and an accuracy improvement of 15.17% after bias removal. This is a significant improvement where this technique shows its potential to be an alternative method for in-situ stress estimation, considering the simplicity of obtaining borehole breakout data from acoustic scanners, rather than performing additional hydraulic or overcoring tests with ancillary equipment.
(3) It is not possible to design underground excavations without knowing the absolute stress magnitudes. This highlights the importance of the proposed technique over conventional stress polygon method (produces a broad range of horizontal stress magnitudes), as it provides reliable estimation on minimum horizontal stress magnitudes.
(4) Moving forward, more breakout experiments have been planned to explicitly quantify the relationship between in-situ stress magnitudes and breakout geometries while obtaining additional data for model training. Field data will also be collected from other mines or oil sites to enrich the validation database. It is expected that with additional data feeding into the ANN model, the prediction accuracy on σ_h will be further increased, and consequently, provide a more reliable in-situ stress estimation technique.

Acknowledgements

The work reported here is funded by Australian Coal Industry's Research Program (ACARP) (No. C26063).

References

[1] Nickless E. Resourcing future generations: A global effort to meet the world's future needs head-on. Eur Geol 2016;42:46–50.
[2] Fairhurst C. Stress estimation in rock: A brief history and review. Int J Rock Mech Min Sci 2003;40(7-8):957–73.
[3] Ljunggren C, Chang Y, Janson T, Christiansson R. An overview of rock stress measurement methods. Int J Rock Mech Min Sci 2003;40(7-8):975–89.
[4] Zoback MD, Moos D, Mastin L, Anderson RN. Wellbore breakouts and in-situ stress. J Geophys Res 1985;90(B7):5523–30.
[5] Barton CA, Zoback MD, Burns KL. In-situ stress orientation and magnitude at the Fenton Geothermal Site, New Mexico, determined from wellbore breakouts. Geophy Res Lett 1988;15(5):467–70.
[6] Zheng Z, Kemeny J, Cook NGW. Analysis of borehole breakouts. J Geophys Res 1989;94:7171–82.
[7] Herrick CG, Haimson BC. Modeling of episodic failure leading to borehole breakouts in Alabama limestone. In: The 1st North American Rock Mechanics Symposium, Austin, Texas 1994.
[8] Haimson B, Lee H. Borehole breakouts and compaction bands in two high-porosity sandstones. Int J Rock Mech Min Sci 2004;41(2):287–301.
[9] Lee H, Moon T, Haimson BC. Borehole breakouts induced in arkosic sandstones and a discrete element analysis. Rock Mech Rock Eng 2016;49(4):1369–88.
[10] Zoback MD, Barton CA, Brudy M, Castillo DA, Finkbeiner T, Grollimund BR, Moos DB, Peska P, Ward CD, Wiprut DJ. Determination of stress orientation and magnitude in deep wells. Int J Rock Mech Min Sci 2003;40(7-8):1049–76.
[11] Chang C, McNeill LC, Moore JC, Lin W, Conin M, Yamada Y. In-situ stress state in the Nankai accretionary wedge estimated from borehole wall failures. Geochem Geophys Geosyst 2010;11(12):n/a–a.
[12] Song I, Chang CD. Stochastic optimization of in-situ horizontal stress magnitudes using probabilistic model of rock failure at wellbore breakout margin. Rock Mech Eng 2018;51(9):2761–76.
[13] Song I. Borehole Breakouts and Core Disking in Westerly Granite: Mechanisms of Formation and Relationship to In-situ Stress. Madison: The University of Wisconsin; 1998.
[14] Zhang H, Yin SD, Aadnoy BS. Poroelastic modeling of borehole breakouts for in-situ stress determination by finite element method. J Petroleum Sci Eng 2018;162:674–84.
[15] Lin H, Kang WH, Oh J, Canbulat I. Estimation of in-situ maximum horizontal principal stress magnitudes from borehole breakout data using machine learning. Int J Rock Mech Min Sci 2020;126:104199.
[16] Shen BT. Borehole breakouts and in situ stresses. In: Proceedings of the First Southern Hemisphere International Rock Mechanics Symposium. Australian Centre for Geomechanics, Perth 2008:407–18.
[17] Zheng ZQ, Kemeny J, Cook NGW. Analysis of borehole breakouts. J Geophys Res 1986;94(B6):7171–82.
[18] Kim H, Xie LM, Min KB, Bae S, Stephansson O. Integrated in situ stress estimation by hydraulic fracturing, borehole observations and numerical analysis at the EXP-1 borehole in Pohang, Korea. Rock Mech Rock Eng 2017;50(12):3141–55.
[19] Martin CD, Martino JB, Dzik EJ. Comparison of borehole breakouts from laboratory and field tests. OnePetro 1994.
[20] Martin CD. Seventeenth Canadian geotechnical colloquium: The effect of cohesion loss and stress path on brittle rock strength. Can Geotech J 1997;34(5):698–725.
[21] Martin CD, Read RS, Martino JB. Observations of brittle failure around a circular test tunnel. Int J Rock Mech Min Sci 1997;34(7):1065–73.
[22] Andersson JC, Martin CD. The Äspö pillar stability experiment: Part I. Experiment design. Int J Rock Mech Min Sci 2009;46(5):865–78.
[23] Andersson JC, Martin CD, Stille H. The Äspö pillar stability experiment: Part II. Rock mass response to coupled excavation-induced and thermal-induced stresses. Int Journal Rock Mech Min Sci 2009;46(5):879–95.
[24] Lin H, Oh J, Canbulat I, Stacey TR. Experimental and analytical investigations of the effect of hole size on borehole breakout geometries for estimation of in-situ stresses. Rock Mech Rock Eng 2020;53(2):781–98.
[25] Mia M, Dhar NR. Prediction of surface roughness in hard turning under high pressure coolant using artificial neural network. Measurement 2016;92:4647–54.
[26] Zain AM, Haron H, Sharif S. Prediction of surface roughness in the end milling machining using artificial neural network. Expert Syst Appl 2010;37(2):1755–68.
[27] Grima MA, Bruines PA, Verhoef PNW. Modeling tunnel boring machine performance by neuro-fuzzy methods. Tunn Undergr Space Technol 2000;15(3):259–69.
[28] Eftekhari M, Baghbanan A, Bayati M. Predicting penetration rate of a tunnel boring machine using artificial neural network. OnePetro 2010.
[29] Mahdevari S, Shahriar K, Yagiz S, Akbarpour SM. A support vector regression model for predicting tunnel boring machine penetration rates. Int J Rock Mech Min Sci 2014;72:214–29.
[30] Elmo D, Stead D. Disrupting rock engineering concepts: Is there such a thing as a rock mass digital twin and are machines capable of learning rock mechanics? Australian Centre for Geomechanics 2020:565–76.
[31] Lin H, Singh S, Oh J, Canbulat I, Kang WH, Hebblewhite B, Stacey TR. A combined approach for estimating horizontal principal stress magnitudes from borehole breakout data via artificial neural network and rock failure criterion. Int J Rock Mech Min Sci 2020;136:104539.
[32] Howard R, Carriquiry AL, Beavis WD. Parametric and nonparametric statistical methods for genomic selection of traits with additive and epistatic genetic architectures. G3: Genes, Genomes. Genetics 2014;4(6):1027–46.
[33] Russell S, Norvig P. Artificial Intelligence: A Modern Approach. London: Prentice hall; 2009.
[34] Yan X, Su XG. Linear Regression Analysis: Theory and Computing. World Scientific; 2009.

[35] Hans C. Bayesian lasso regression. Biometrika 2009;96(4):835–45.
[36] Marquardt DW, Snee RD. Ridge regression in practice. Am Stat 1975;29 (1):3–20.
[37] Kleinbaum DG, Klein M, Pryor ER. Logistic Regression: A Self-learning Text. New York: Springer; 2010.
[38] Murphy KP. Naive Bayes Classifiers. University of British Columbia 2006;18:1–8.
[39] Burba F, Ferraty F, Vieu P. *k*-Nearest Neighbour method in functional nonparametric regression. J Nonparametric Stat 2009;21(4):453–69.
[40] Loh WY. Classification and Regression Tree Methods. In: Encyclopedia of Statistics in Quality and Reliability 2008;1:315–23.
[41] Svetnik V, Liaw A, Tong C, Culberson JC, Sheridan RP, Feuston BP. Random forest: A classification and regression tool for compound classification and QSAR modeling. J Chem Inf Comp Sci 2003;43(6):1947–58.
[42] Cortes C, Vapnik V. Support-vector networks. Mach Learn 1995;20(3):273–97.
[43] Chu W, Ghahramani Z, Williams CK. Gaussian processes for ordinal regression. J Mach Learn Res 2005;6.
[44] Hopfield JJ. Artificial neural networks. IEEE Circuits and Devices Mag 1988;4 (5):3–10.
[45] Walton G, Kalenchuk KS, Hume CD, Diederichs MS. Borehole breakout analysis to determine the in-situ stress state in hard rock. San Francisco, California: Rock Mechanics/Geomechanics Symposium; 2015.
[46] Shen B. Borehole Breakouts and In-situ Stresses. In: Proceedings of the First Southern Hemisphere International Rock Mechanics Symposium, Australian Centre for Geomechanics; 2008, p. 407–18.
[47] Klee G, Bunger A, Meyer G, Rummel F, Shen B. In-situ stresses in borehole Blanche-1/South Australia derived from breakouts, core discing and hydraulic fracturing to 2 km depth. Rock Mech Rock Eng 2011;44(5):531–40.
[48] Shen B, Rinne M. Estimate in-situ stresses from borehole breakout at Blanche-1 geothermal well in Australia. ITA-AITES World Tunnel Congress 2011:414–5.
[49] LeRiche AC. Stress estimation from borehole scans for prediction of excavation overbreak in brittle rock. Master's Dissertation. Queen's University; 2017.
[50] Haimson BC. Borehole breakouts and in-situ stress. 12th Annual Energy-sources Technology Conference and Exhibition, Houston, New York, American Society of Mechanical Engineers; 1989, p. 17–22.
[51] Lin H, Oh J, Canbulat I, Hebblewhite B, Masoumi H, Walsh S. Experimental study on borehole size effect and prediction of breakout initiation stress. Int J Rock Mech and Min Sci 2021;142:104762.